Baseline Estimation for Repeat-Pass Interferometric Synthetic Aperture Sonar

Jeremy Dillon
Kraken Sonar Systems Inc.
St. John's, NL, Canada
jdillon@krakensonar.com

Vincent Myers
Defence R&D Canada – Atlantic
Dartmouth, NS, Canada
vincent.myers@drdc-rddc.gc.ca

***Abstract*— Synthetic aperture sonar has the potential to create extremely detailed maps of seafloor topography when repeated passes are flown at different altitudes to create a long interferometric baseline. However, navigation uncertainty typically limits the accuracy of the baseline measurement which is required to convert interferometric phase to seafloor depth. We present a data-driven baseline estimator and experimental results for the case where repeated passes are flown with an interferometric sonar consisting of two vertically displaced arrays. It is shown that co-registration of repeat-pass imagery and bathymetry alleviates the need to post-process data from a high grade inertial navigation system.**

***Index Terms*— synthetic aperture sonar, bathymetry, baseline, repeat-pass, interferometry.**

I. Introduction

Seabed mapping is a key activity for many underwater applications such as offshore oil and gas exploration, pipeline surveying, ocean science, mine warfare, and hydrography. Synthetic Aperture Sonar (SAS) is a a technique for creating high resolution seabed imagery that shares many similarities with Synthetic Aperture Radar (SAR). The forward motion of the sonar platform is used to synthesize an array that is much longer than the physical length by combining multiple pings in software. Thus, SAS uses signal processing to circumvent the usual trade-off between range, array length, and wavelength in conventional sonar. The result is an along track resolution proportional to the transmitter length and independent of both range and frequency.

In addition to reflectivity images, sonar can produce topographic maps of the seafloor by detecting the angle of arrival of seabed echoes coming from a given range bin. In a configuration known as Interferometric SAS (InSAS), two vertically separated sonar receiver arrays enable the production of bathymetric maps that are exactly co-registered with the SAS imagery because the bathymetry is derived by cross-correlating SAS images from each array [1]. This combination of synthetic aperture processing and interferometric processing solves the problems of limited resolution and coverage rates encountered with conventional swath bathymetric sonars and multibeam echo sounders. The capability of generating centimetre-scale resolution in three dimensions is especially interesting for mine warfare because 3D imaging has the potential to provide significant improvements in the detection, classification, and identification of small seabed objects [2].

The sensitivity of an interferometer is determined by its baseline, which is defined as the distance between elements of the array. For single-pass interferometry, the baseline is limited by the physical dimensions of the sonar platform such as the hull diameter of an Autonomous Underwater Vehicle (AUV) or tow-fish. As InSAS baselines are typically on the order of 20 to 30 wavelengths [3, 4], the interferometric correlation must be averaged over multiple pixels to achieve satisfactory results, resulting in a trade-off between horizontal resolution and vertical accuracy.

A baseline on the order of hundreds or thousands of wavelengths can be realized by combining SAS images from repeated passes that are intentionally flown at different altitudes. Repeat-pass interferometry has been extensively studied in the context of spaceborne SAR to create a Digital Elevation Model (DEM) for the Earth's surface [5]. For SAS, interest in repeat-pass interferometry has primarily been driven by the challenge of detecting targets in highly cluttered environments [6], although there have been limited attempts to obtain topographic information from repeat-pass AUV missions [7]. In spaceborne SAR, the interferometric baseline is typically estimated from orbital measurements, from ground points of known height [8], or from Fourier analysis of the interferometric phase assuming a known DEM [9]. However, none of these techniques is applicable to SAS because underwater navigation measurements are of limited accuracy and the seabed topography is a priori unknown.

In this paper, we present a simple method for estimating the repeat-pass baseline using the complex SAS images and the InSAS height maps from each pass. The method can be applied to any InSAS without requiring access to raw acoustic data or for post-processing data from a high grade inertial navigation system (unlike, for example, the technique in [10] that requires images to be re-focused five times). Additionally, the method is sufficiently simple to implement that it raises the interesting possibility of performing baseline estimation and 3D target reconstruction in near real-time onboard an AUV as part of an adaptive concept of operations for target detection and classification.

Financial support for J. Dillon was provided by the Natural Sciences and Engineering Research Council of Canada and the Research and Development Corporation of Newfoundland and Labrador.

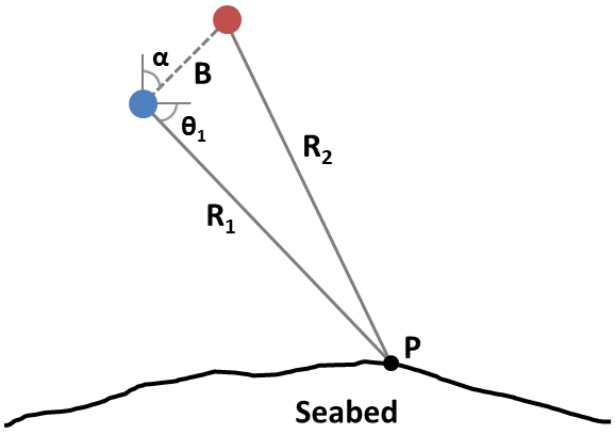

Fig. 1. Typical geometry of across track interferometry. The grey solid lines indicate the range from an arbitrary point **P** on the seabed to the position of the sonar on subsequent passes 1 (blue) and 2 (red). The baseline is denoted by the dashed line **B**.

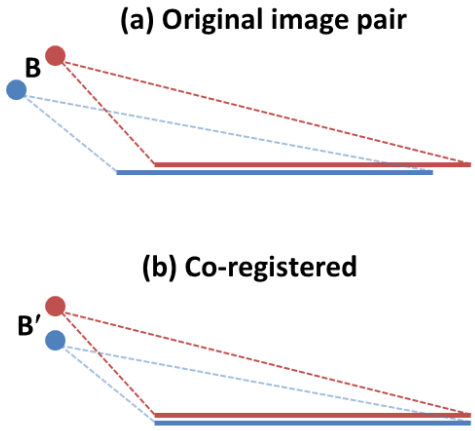

Fig. 2. Image pairs before and after co-registration. In (a), **B** represents the baseline vector between the synthetic apertures of each image. In (b), the residual baseline vector $\mathbf{B}'$ is vertical after co-registration.

II. Theory

A. Interferometry

The geometry of across track interferometry is shown in Figure 1, where the blue and red dots represent the positions of the sonar on passes 1 and 2, respectively, and the baseline is denoted by the dashed line **B**. The vectors $\mathbf{R}_1$ and $\mathbf{R}_2$ represent the locations of the sonar relative to the position of an arbitrary point **P** on the seabed. The angle α denotes the tilt of the baseline with respect to vertical, and θ_1 represents the elevation angle of $\mathbf{R}_1$ as seen from **P**.

When the seabed echoes from **P** are cross-correlated, the interferometric phase ϕ is given by [5]

$$\phi = \frac{4\pi}{\lambda}\Delta R \tag{1}$$

where λ is the acoustic wavelength, ΔR is the path length difference $R_2 - R_1$, and in practice ϕ can only be measured modulo 2π radians. If we take 1 as a reference location and make the assumption that $B \ll R$, then $\mathbf{R}_1$ and $\mathbf{R}_2$ are approximately parallel and the elevation angle at 1 is

$$\theta_1 = \alpha + \arcsin\frac{\Delta R}{B}. \tag{2}$$

The arcsin term represents the angle of arrival across the interferometer and B is the length of the vector **B**. Combining (1) and (2), the vertical distance between **P** and 1 is

$$\begin{aligned} h_1 &= R_1 \sin\left(\alpha + \arcsin\frac{\phi\lambda}{4\pi B}\right) \\ &\approx \frac{R_1\phi}{4\pi}\frac{\lambda}{B}\cos\alpha. \end{aligned} \tag{3}$$

where (3) represents a small angle approximation for the angle of arrival. The interferometric phase therefore provides a measurement of the height h above the seabed, with the sensitivity of the interferometer being proportional to the baseline length expressed in units of acoustic wavelengths.

In Figure 1, the baseline **B** is a 3D vector time series that represents the difference in sonar position between passes. However, during synthetic aperture image formation, images are focused by time-shifting the echoes from individual pings to account for nonlinear deviations in the platform trajectory [11]. Therefore, when repeat-pass interferometry is performed using synthetic aperture images, the path length difference in (1) is the difference with respect to *synthetic* trajectories, and **B** is the corresponding difference between the synthetic apertures formed on each pass.

The expression for the interferometric phase in (1) is essentially a narrow bandwidth formulation. In practice, a sonar transmits a pulse of bandwidth β to achieve a range resolution of $c/2\beta$, where c is the sound speed in water. Typical along track and across track resolutions are on the order of a few centimetres for a high resolution SAS. The images from repeated passes must be co-registered to within a fraction of a resolution cell to ensure coherence.

The geometry of the image pairs before and after co-registration is shown in Figure 2. Image co-registration eliminates the horizontal (i.e., along track and across track) baseline components between synthetic trajectories. When each pass is flown with an InSAS rather than a SAS, the residual vertical component $\mathbf{B}'$ can be estimated by comparing the interferometric height estimates from each pass. Relative height maps h_1 and h_2 can be formed by applying (3) to the single-pass cross-correlation of SAS images from each row of the InSAS. The along track variation of the vertical baseline is then obtained by averaging the difference of co-registered height maps in the across track direction, i.e.

$$\mathbf{B}' = \frac{1}{y_{\max} - y_{\min}}\int_{y_{\min}}^{y_{\max}} (h_2 - h_1)\, dy, \tag{4}$$

where y denotes the across track ground range coordinate.

Fig. 3. Deployment of the Arctic Explorer AUV in Bedford Basin, Nova Scotia. The AquaPix transducer array is installed in the payload section aft of the nose cone.

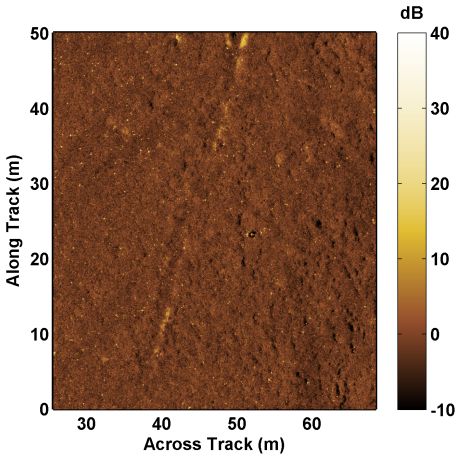

Fig. 4. AquaPix SAS seabed image of the region selected for repeat-pass analysis. The image is from the survey at 14.5 m altitude.

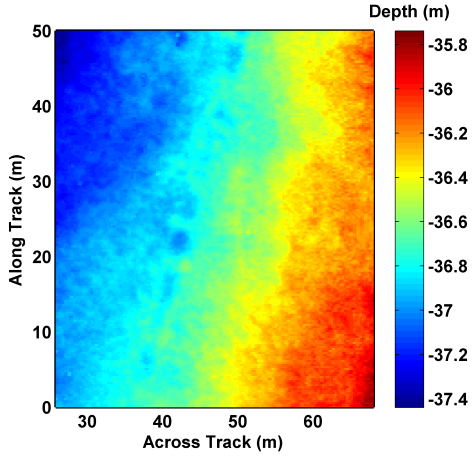

Fig. 5. AquaPix InSAS bathymetry corresponding to the SAS image in Figure 4. The vehicle depth has been added to the InSAS relative height measurement to show the depth of the seabed relative to the surface.

III. Experimental Results

A. Sea trial

AquaPix® is a wideband 300 kHz interferometric SAS featuring a unique dual row design for multipath suppression [3]. The sonar was integrated into an Arctic Explorer AUV manufactured by International Submarine Engineering [12]. As shown in Figure 3, the vehicle was deployed from a jetty at the Bedford Institute of Oceanography to collect survey data in Bedford Basin, Nova Scotia, for a joint research project on repeat-pass interferometry with Defence Research and Development Canada (DRDC).

One of the objectives was to determine the maximum allowable separation between passes by measuring the coherence as a function of altitude. A series of rectangular circuits were flown at altitudes of 12.7, 12.9, 13.6, 14.5, and 17.2 m, resulting in 10 repeat-pass image pairs with 9 distinct baseline lengths (the altitude difference of 0.9 m occurs twice). Figure 4 shows a SAS seabed image from the 14.5 m pass generated by Kraken's GPU-accelerated imaging software, which is part of the company's INSIGHT software suite. The corresponding bathymetric map from single-pass interferometry is shown in Figure 5, where the vehicle depth has been added to the InSAS relative height measurement to show the depth of the seabed relative to the sea surface. The mean seabed slope is 1.4°. It can be seen that the selected region is generally flat and featureless, except for a faint scour mark running diagonally across the image.

B. Baseline estimation

The mean estimates of the residual vertical baselines after repeat-pass InSAS co-registration are shown in Figure 6, along with the corresponding mean altitude differences measured by the on-board altimeter and Doppler Velocity Log (DVL). The abscissa indicates the nominal baseline for each image pair, which is defined as the difference between the altitude set points that were programmed into the vehicle controller. The grey line in Figure 6 represents the line $y = x$ denoting the expected baseline measurement for each image pair. However, the vehicle control system did not always follow the programmed altitude exactly, which is evident from the upward trend of measurements for the larger baselines.

The results in Figure 6 show consistent agreement to within about 10 cm between the InSAS baseline estimates and the altitude measurements from two independent sensors. The means and standard deviations of differences between each pair of estimates are shown in Table I. It is worth emphasizing that neither altitude sensor can be considered as ground truth when performing interferometry with SAS images that have been formed relative to the ideal linear track of a synthetic aperture. The SAS image co-registration for horizontal baseline estimation resulted in across track offsets between repeated passes of up to 5 m. Heading differences between passes were 0.6° or less, and these differences were eliminated during co-registration using truncated sinc interpolation. The magnitudes of the InSAS mean differences in Table I are less than the 1σ levels, indicating that there is no observed bias in the InSAS baseline estimation technique.

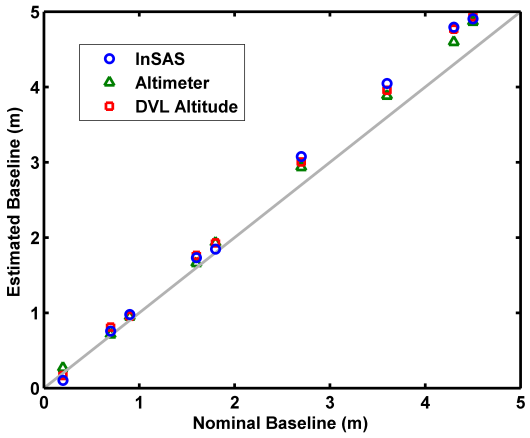

Fig. 6. Comparison of the mean vertical baselines estimated from repeat-pass InSAS co-registration and altitude differences measured by the altimeter and DVL on-board the vehicle.

TABLE I

MEAN AND STANDARD DEVIATION OF BASELINE DIFFERENCES.

Difference	Mean (cm)	Std. Dev. (cm)
InSAS – Altimeter	3.3	12.1
InSAS – DVL	−1.4	6.6
Altimeter – DVL	−4.7	7.6

IV. CONCLUSION

In this paper, a simple method has been presented for estimating the baseline between repeated passes of an interferometric SAS. The method allows estimation at the centimetre-scale without need for deploying reference targets, reprocessing SAS images, or post-processing data from an inertial navigation system. Computational efficiency results from only requiring the co-registration of two complex SAS images and averaging of the corresponding InSAS bathymetric maps. Since SAS images can be focused using relatively low cost angular rate sensors, the method is suitable for vehicles lacking a high grade navigation system, or for the case where raw data is unavailable for post-processing.

Results were presented for AquaPix, a wideband 300 kHz interferometric SAS that was integrated into an Arctic Explorer AUV for sea trials in Bedford Basin, Nova Scotia. Experimental results indicated that estimates of the mean vertical baseline were consistent with independent measurements from an altimeter and a DVL over a range of up to 5 m, which corresponds to an interferometric spacing of up to 1000 wavelengths. The agreement shown in Figure 6 was found to be insensitive to the content of the seabed image. For example, the presence of the scour mark in Figure 4 was not necessary for co-registration of the repeat-pass images since cross-correlation of complex SAS images results in a sharp correlation peak even in the limiting case of a perfectly uniform seabed consisting of uncorrelated point scatterers.

The image co-registration method used for horizontal baseline estimation is accurate to within a fraction of the SAS image resolution, which is on the order of 3 cm for high resolution systems such as AquaPix. Unfortunatley, there is no readily available ground truth instrumentation for evaluating the vertical separation between two synthetic apertures. Therefore, the merit of the baseline estimation method will ultimately be evaluated in ongoing work by unwrapping the phase of the repeat-pass interferogram and examining the corresponding bathymetric map for targets of known height.

ACKNOWLEDGMENT

We thank the PISCES2 team from DRDC Atlantic, the Canadian Navy, the Bedford Institute of Oceanography, and Kraken Sonar Systems for supporting the SAS sea trial.

REFERENCES

[1] H. Callow, P. Hagen, R. Hansen, T. Sæbo and R. Pedersen, "A new approach to high-resolution seafloor mapping," Mapping the Ocean, vol. 7, no. 2, 2012, pp. 13–22.

[2] F. Florin, F. Fohanno, I. Quidu and J.-P. Malkasse, "Synthetic aperture and 3D imaging for mine hunting sonar," in Proc. Undersea Defence Technology (UDT) Europe, Nice, France, June 23–25, 2004, pp. 1–20.

[3] M. Pinto, "Interferometric synthetic aperture sonar design optimized for high area coverage shallow water bathymetric survey," in Proc. Underwater Acoustic Measurements, Kos, Greece, June 20–24, 2011, pp. 1–7.

[4] T. Sæbo, "Seafloor depth estimation by means of interferometric synthetic aperture sonar," Ph.D. dissertation, University of Tromsø, Norway, 2010.

[5] R. Bamler and P. Hartl, "Synthetic aperture radar interferometry," Inverse Problems, vol. 14, 1998, pp. R1–R54.

[6] V. Myers, I. Quidu, T. Sæbo and R. Hansen, "Results and analysis of coherent change detection experiments using repeat-pass synthetic aperture sonar images," in Proc. Underwater Acoustic Measurements, Corfu, Greece, June 23–28, 2013, pp. 613–620.

[7] R. De Paulis *et al.,* "SAS multipass interferometry for monitoring seabed deformation using a high-frequency imaging sonar," in Proc. IEEE OCEANS, Santander, Spain, June 6–9, 2011, pp. 1–10.

[8] H. Kimura and M. Todo, "Baseline estimation using ground points for interferometric SAR," in Proc. IEEE IGARSS, Singapore, August 3–8, 1997, pp. 442–444.

[9] K. Singh, N. Stussi, K. L. Keong and L. Hock, "Baseline estimation in interferometric SAR," in Proc. IEEE IGARSS, Singapore, August 3–8, 1997, pp. 454–456.

[10] T. Sæbo, R. Hansen, H. Callow and S. Synnes, "Coregistration of synthetic aperture sonar images from repeated passes," in Proc. Underwater Acoustic Measurements, Kos, Greece, June 20–24, 2011, pp. 1–8.

[11] A. Bellettini and M. Pinto, "Theoretical accuracy of synthetic aperture sonar micronavigation using a displaced phase-center antenna," IEEE Journal of Oceanic Engineering, vol. 27, no. 4, 2002, pp. 780–789.

[12] T. Crees *et al.,* "UNCLOS under ice survey – An historic AUV deployment in the Canadian high arctic," in Proc. OCEANS 2010 Conference, Seattle, WA, September 20–23, 2010, pp. 1–8.